



ENVIRONMENTAL HEALTH PERSPECTIVES

<http://www.ehponline.org>

Validating Satellite-Derived Land Surface Temperature with *in Situ* Measurements: A Public Health Perspective

Jalonne L. White-Newsome, Shannon J. Brines,
Daniel G. Brown, J. Timothy Dvonch, Carina J. Gronlund,
Kai Zhang, Evan M. Oswald and Marie S. O'Neill

<http://dx.doi.org/10.1289/ehp.1206176>

Online 7 June 2013

Validating Satellite-Derived Land Surface Temperature with *in Situ* Measurements: A Public Health Perspective

Jalonne L. White-Newsome¹, Shannon J. Brines², Daniel G. Brown², J. Timothy Dvonch¹,
Carina J. Gronlund¹, Kai Zhang⁴, Evan M. Oswald³, and Marie S. O'Neill^{1,5}

¹University of Michigan School of Public Health, Ann Arbor, Michigan, USA

²University of Michigan School of Natural Resources and Environment, Ann Arbor, Michigan,
USA

³ University of Michigan Department of Atmospheric, Oceanic and Space Sciences, Ann Arbor,
Michigan, USA

⁴University of Texas School of Public Health, Division of Epidemiology, Human Genetics and
Environmental Sciences, Houston, Texas, USA

⁵University of Michigan Risk Science Center, Ann Arbor, Michigan, USA

Corresponding Author (current address):

Dr. Jalonne L. White-Newsome

WE ACT for Environmental Justice

50 F St, NW, 8th Floor

Washington, DC 20001

Jalonne@weact.org

Running Title: Validating satellite temperature measurements

Key Words: epidemiology, ground truthing, heat, Landsat satellite, land surface temperature,
remote sensing, surface imperviousness, temperature, urban areas

CFI Statement: The authors declare that they have no actual or potential competing financial interests.

Acknowledgements

This work was supported by: the National Occupational Research Agenda Pre-Doctoral Scholarship from the University of Michigan Center for Occupational Health and Safety Engineering, a National Institute for Occupational Safety and Health (NIOSH)-funded Education and Research Center, NIOSH grant 2T42OH008455; the U.S. Environmental Protection Agency Science to Achieve Results (STAR) grant R832752010; the National Institute of Environmental Health Sciences grant R01ES016932; U.S. Centers for Disease Control and Prevention grant R18EH000348; and the University of Michigan Graham Environmental Sustainability Institute. Carina J. Gronlund was supported by the National Institute on Aging Interdisciplinary Research Training in Health and Aging grant T32AG027708. Jalonne L. White-Newsome was supported by the Kendall Science Fellowship with the Union of Concerned Scientists.

Abbreviations/Definitions

ASTER:	Advanced Spaceborne Thermal Emission and Reflection Radiometer
Buffer:	Circular area (with a specified radius of 0-800 meters (m)) centered around an outdoor temperature monitoring unit
Emissivity:	The ratio of the radiation emitted by a surface to the radiation emitted by a blackbody at the same temperature, i.e., how well different surfaces reflect solar energy
GIS:	Geographic Information Systems
HHWS:	Heat Health Warning System
L5-TM:	the Landsat-5 satellite Thermal Mapper

LST:	Land Surface Temperature, on-the-ground temperature estimate derived from L5-TM measurements
MODIS:	Moderate Resolution Imaging Spectroradiometer
NDVI:	Normalized Difference Vegetative Index
NLCD:	National Land Cover Dataset
NOAA-AVHRR:	National Oceanic and Atmospheric Administration Advanced Very High Resolution Radiometer
SI:	Percent surface imperviousness, percentage of surface impenetrable by water
USGS:	United States Geological Survey

Abstract

Background: Land surface temperature (LST) and percent surface imperviousness (SI), both derived from satellite imagery, have been used to characterize the urban heat island effect, a phenomenon in which urban areas are warmer than non-urban areas.

Objectives: We aimed to assess the correlations between LSTs and SI images with actual temperature readings from a ground-based network of outdoor monitors.

Methods: We evaluated the relationships between 1) LST calculated from a 2009 summertime satellite image of the Detroit Metropolitan Region, Michigan, 2) SI from the 2006 National Land Cover Data Set, and 3) ground-based temperature measurements monitored during the same time period at 19 residences throughout the Detroit Metropolitan Region. Associations between these ground-based temperatures and the average LSTs and SI at different radii around the point of the ground-based temperature measurement were evaluated at different time intervals. Spearman correlation coefficients and corresponding p-values were calculated.

Results: Satellite derived LST and SI values were significantly correlated with 24-hour average and August monthly average ground temperatures at all but 2 of the radii examined (100 m for LST and 0 m for SI). Correlations were also significant for temperatures measured between 4:00 and 5:00 a.m. for SI, except at 0 m, but not LST. Statistically significant correlations ranging from 0.49 to 0.91 were observed between LST and SI.

Conclusions: Both SI and LST could be used to better understand spatial variation in heat exposures over longer time frames but are less useful for estimating shorter term, actual temperature exposures, which can be useful for public health preparedness during extreme heat events.

INTRODUCTION

Use of thermal remote sensing and advanced spatial modeling are emerging trends in the field of environmental epidemiology and public health. Geospatial technologies provide a valuable resource to assist public health practitioners and emergency response planners in identifying areas that are most at risk and using these scientific outputs to inform policies and practices. Thermal remote sensing products such as thermal images captured by the Landsat-5 Thermal Mapper (L5-TM) instrument have been used to study areas of higher relative temperatures within a city, also known as micro-urban heat islands (Johnson 2009).

L5-TM has an advantage over other sensors, like the Moderate Resolution Imaging Spectroradiometer (MODIS) (<http://modis.gsfc.nasa.gov/about/>) (MODIS 2011), in that L5-TM provides a spatial resolution of 120 m (compared to 1000 m for the thermal band of MODIS), though it provides only 16-day repeatability, at best, compared to 1-day for MODIS (Aniello et al. 1995). Advanced Spaceborne Thermal Emission and Reflection Radiometer (ASTER) is another sensor that could be used but imagery is not available free of charge (<http://asterweb.jpl.nasa.gov/>) (NASA 2012). The data captured by satellite can be transformed into several helpful measures, including land surface temperatures (LST) and percent surface imperviousness (SI). LSTs are a primary factor in determining surface radiation and human comfort in cities (Weng 2009).

The higher spatial resolution of L5-TM information is important in micro-urban heat island studies, so we focus on those data here. The SI is defined as the percent of the surface of an area that is not penetrable by water, such as concrete or asphalt, and can be mapped at a 30-meter resolution with L5-TM. This characteristic has been commonly used in studies to assess the

degree of urbanization of an environment as well as explore the spatial extent of surface urban heat islands (Roy and Yuan 2009).

The relationship between LST and vegetated areas has been documented in the literature. A study by Aniello and colleagues compared the spatial distribution of micro-urban heat islands and tree cover in Dallas, Texas using L5-TM and GIS (Aniello et al. 1995). They examined the usefulness of L5-TM for classifying tree-cover information and using thermal band 6 to produce a thermal map of Dallas. Their methods involved processing and classifying L5-TM images and tree cover data in GIS. While L5-TM data was useful for mapping micro-urban heat islands in Dallas, the authors recommended use of exact on-the-ground temperatures for image calibration in future studies. Remote sensing data have been used to help model urban surface temperatures; specifically, validating LST data with actual on-the-ground temperature measurements, known as ground-truthing. For example, strong correlations between satellite-derived air temperatures and in situ measurements were found when characterizing urban heat island intensity in Hong Kong, using Advanced Spaceborne Thermal Emission and Reflection Radiometer (ASTER) satellite imagery (Fung et al. 2009). Comparisons between ground temperatures and estimated temperatures using imagery from MODIS, the National Oceanic and Atmospheric Administration Advanced Very High Resolution Radiometer (NOAA-AVHRR) and Landsat TM, showed a very high correlation in both urban and rural areas (Rigo et al. 2006). While previous studies have used Landsat to create prediction models for surface temperature, and shown strong correlations between surface temperature and surface imperviousness (Cheung et al, 2002), few studies have simultaneously explored the relationship between SI, ground-based temperature measures and LST calculated from thermal imagery.

Adaptation to the consequences of climate change, as future scenarios of heat-related morbidity and mortality become a major public health concern, requires predicting areas of high vulnerability to heat in cities. Epidemiologic studies on heat and health have begun to use satellite-derived temperatures (instead of temperature data from the nearest airport) and land cover to potentially provide more refined heat exposure classifications. A study in Philadelphia used geographic information systems (GIS) and thermal imaging to investigate the relationship between the spatial distributions of vulnerable populations, urban heat island intensities and heat-related deaths (Johnson and Wilson 2009). This study recommended that more multi-year studies use spatial modeling and remote sensing methods to better help determine areas of risk throughout cities

Uejio and colleagues used Landsat TM and ETM+ data to determine the magnitude and spatial variation of mean radiant surface temperature for different densities of impervious surface area (ISA), to further document the change in air trends and air quality that can result from transforming land use from rural to urban (Uejio et al. 2011). Harlan and colleagues used Landsat (30 meter resolution) to calculate NDVI and estimated surface temperatures (Harlan et al. 2012).

There is still a need to understand how proxies for heat exposure correlate with actual heat exposure. Harlan and colleagues provide correlations between the mean NDVIs and surface temperatures at the Census block group level. Our study goes beyond this comparison by correlating SI, land surface temperature (estimated from Landsat) and actual temperature measurements made by a ground-based temperature monitor network over the summer. Our study is novel for evaluating the correlations between satellite-derived temperatures and a ground-based temperature network with high temporal (10 minutes) and spatial resolution (19

monitors over a range of levels of SI within a single county) at a height relevant to human health (1.5 meters above the ground). Further, it characterizes these features in metropolitan Detroit, Michigan, USA, a location where people may be poorly adapted to heat and several epidemiologic studies have already shown important and socially unequal health consequences associated with hot weather (O'Neill et al. 2003; Schwartz et al. 2004; Sheridan and Kalkstein 2010, Anderson and Bell 2009).

Indeed, integrating information from ground-based temperature monitoring networks and satellite-derived images using a GIS platform can provide useful data for exposure assessments in most urban areas, specifically for the study of heat-related death and illness. Validation of satellite data sources by ground-truthing can help characterize and identify neighborhood-level urban heat islands, which could be useful for public health professionals and urban planners to prevent heat-related mortality and other adverse health effects from high summer temperatures. This type of data could also direct intervention strategies to reduce the urban heat island effect. Some previously published work did not explicitly address the practical challenges of integrating insights from ground-truthing studies with public health research and applications (Lo and Faber 2003).

The purpose of this study is to apply a public health perspective to a determination of whether spatial variation of temperatures within a network of ground-based outdoor temperature monitors is correlated with satellite derived LST and SI. Although we did not expect LST (which represents the temperature of the ground) to completely predict the temperature of the air at a height relevant to human health, we hypothesized that the air temperatures measured by a ground-based temperature monitoring network would be highly correlated with LST, as well as values of SI.

METHODS

Ground based temperature monitoring network and surface imperviousness

Sites in our ground-based temperature monitor network in the Detroit metropolitan region (Wayne County, Michigan) were selected with site SI values ranging from 0 to 100 percent imperviousness with buffer zones around each site ranging from 0 to 800 meters.. We picked both urban and rural locations to assess the temperature differences amongst areas within the same county that might have different land-use patterns. This strategy was, in part, designed to evaluate the existence of urban heat island structure in the Detroit metropolitan region (Oswald et al. 2012; Zhang et al. 2011). Using SI from the United States Geologic Survey (USGS) NLCD product (MRLC 2013) (<http://www.mrlc.gov/nlcd2006.php>), half-mile smoothing of every pixel was performed and SI was classified by decile. Once the SI surrounding various prospective residential sites for placing the temperature monitors was established and a range of SI levels was ensured by the sampling strategy, home occupants were approached, explained the purpose of the study and asked if they would be willing to have a temperature monitor outside their homes. All volunteers signed an agreement letter to participate. The research was compliant with all relevant national, state and local human subjects regulations.

HOBO Pro v2 U23-002 (external temperature/relative humidity) outdoor temperature monitoring devices from the Onset corporation [Onset HOBO Data Loggers, Pocasset, MA] were calibrated and used to record temperature and relative humidity at 10-minute intervals from June 13 to September 30, 2009. The calibration process involved collocating the monitors in a controlled environment along with a temperature probe from the National Institute of Standards and Technology to ensure that the temperatures recorded were within the accuracy range reported in

the operation manual, i.e. $\pm 0.21^{\circ}$ C, within an ambient temperature range of 0 to 50° C (http://www.onsetcomp.com/files/manual_pdfs/10694-K-MAN-U23.pdf) (ONSET 2013). Monitors were positioned in residential grass-covered backyards of volunteers following a strict placement protocol that required monitors to be sited at least 10 feet (3 m) away from buildings, homes and trees; 1.5 m from the actual surface [to better assess the level of exposure that would be experienced by a person of average height and to be consistent with the instrument siting protocols used by The World Meteorological Organization, as well as NOAA's National Weather Service (WMO 2008)]; not in the direct pathway of automatic lawn sprinkling systems; not in a shady area or near falling objects; away from power lines and swampy damp ground; and facing southwest.

Processing the LANDSAT L5-TM satellite image to derive land surface temperature

Images of the Earth were taken nearly continuously from March 1, 1984 to November 2011 on a 16-day cycle by the L5-TM, which consistently imaged the Detroit Metropolitan Region at about 12:05 p.m. Eastern Daylight Time (EDT) at each pass. L5-TM captured images collected at a 705 km altitude, 185 km swath, 120-m spatial resolution for thermal band data and 30-m resolution for the other spectral bands. The satellite images captured by L5-TM are free and downloadable from the USGS at <http://earthexplorer.usgs.gov/> (USGS 2013).

Satellite images were downloaded for use only if they met the following criteria: the images were captured during the study period; covered the entire study area (geographically); had less than 14% cloud cover and were taken under clear weather conditions. More cloud cover and unclear weather conditions can inhibit the signal strength reflected back to the satellite and cause underestimation of the ground surface temperature. Each image had 7 spectral bands of

information. Thermal infra-red band 6 (10.4 - 12.5 μm) provides the data that can be converted from raw digital numbers to LST. To convert from a digital number to a temperature, calibration formulas, atmospheric correction tools and transformations were necessary (Figure 1). Once an image was selected by our criteria, ERDAS Imagine 9.2 software (Leica Geosystems, Inc., Atlanta, Georgia) was used to convert the image (from a TIFF file to an IMG file) to a usable format for GIS. ArcGIS v9.3.1 (ESRI, Redlands, CA) was used to perform the calculations outlined below. First we converted the digital numbers taken from the raw image into at-sensor spectral radiance (L_{TOA} , the temperature read at the sensor, $\text{W}/\text{m}^2 \cdot \text{sr} \cdot \mu\text{m}$). The source equations and calibration constants developed specifically for L5-TM images were used from the process outlined by G. Chander (Chander et al. 2009). L_{TOA} was then used to calculate an actual ground surface temperature.

Because the satellite signal received by the sensor is in space, the effects of the atmosphere (i.e. air pollution, weather) and surface emissivity (the ratio of the radiation emitted by a surface to the radiation emitted by a blackbody at the same temperature, i.e. how well different surfaces reflect solar energy) can have considerable influence on the accuracy of the satellite-derived surface temperature. To account for these influences, we used a tool which estimates atmospheric influences in conjunction with a data layer of emissivity for the study area. Using this web-based atmospheric correction parameter tool developed by Barsi et al. located at <http://atmcorr.gsfc.nasa.gov/> (Barsi et al. 2003) we estimated 3 scene specific parameters for each satellite image. The tool required the following inputs for each satellite scene: year, month, day, Greenwich Mean Time (GMT) and latitude and longitude coordinates. The outputs of this tool were the 3 parameters: atmospheric transmission (T , unitless), upwelling radiance (L_u ,

$W/m^2 \cdot sr \cdot \mu m$) and downwelling radiance (L_d , $W/m^2 \cdot sr \cdot \mu m$) where $W/m^2 \cdot sr \cdot \mu m$ are the units of spectral radiance: watts per square meter per steradian per micrometer.

Values of emissivity for the study area were then estimated by examining the land use/land cover designations, downloaded for the region from the 2006 NLCD. We considered the differences in emissivity of various impervious surface land cover types in the main equation to calculate surface temperature. Because our land-cover data does not distinguish among different types of impervious surface, we were unable to represent possible differences in emissivities among them. We created a layer of emissivity (ϵ , range 0 to 1) for the study area based on reference emissivity values for various landcover classes used in other studies (Lillesand et al. 2008). These values of emissivity, coupled with the atmospheric correction parameters, were used in the following equation to calculate the radiance of a blackbody target of kinetic temperature (L_T), which ultimately represented surface temperature:

$$L_T = (L_{TOA} - L_u - (1 - \epsilon) \cdot L_d) / (T \cdot \epsilon), \quad [1]$$

where L_T = Radiance of a blackbody target of kinetic temperature and L_{TOA} = at sensor spectral radiance, $W/m^2 \cdot sr \cdot \mu m$. We then transformed L_T into a temperature in Kelvin (using Planck's equation), and then converted Kelvin to $^{\circ}C$.

Once the scene was transformed to a surface temperature in units of $^{\circ}C$, temperatures outside our range of interest (below $0^{\circ}C$) or areas of no data (water) were masked out of the layer (given a value of NoData). The implausible ranges were likely a result of some cloud cover over a certain point, values over a body of water, or possibly a source of error in the reflectance value that would cause noise in the analysis.

Geographical and statistical analysis

Using spatial analysis tools in ArcGIS, the LST and SI were averaged over the areas of the following 7 concentric circles with different radii around each outdoor monitoring unit (buffers): at the point (0 m), 100, 200, 300, 400, 500, and 800 m. We assessed the values at different buffers because they can be representative of physical processes that can occur at different spatial scales within the urban canopy layer, the layer of the urban atmosphere extending upward from the surface to building height (Roy and Yuan 2009). These spatial scales range from the micro-level (at the home = 0 m) to more macro-level (block, neighborhood) exposures. The physical mechanism of correlation is that thermometers 'sense' temperature that is transferred from the 'source area' (i.e. surfaces below, around) to the sensors through turbulent transport. Thus the relationship between source area (i.e. LST) and thermometer is dependent on both atmospheric and surface states. Furthermore, LST and ground-based temperature can be influenced by a number of physical factors relevant to the study area: surface heterogeneity, considerable variability in temperature over small areas, and physical structures, and the varying buffers allowed exploration of on what scale these factors might operate. From a health perspective, understanding correlations at these different spatial scales can inform tools for use at the urban-local scale, to predict 'hot spots' where prevention of heat illness and deaths is especially needed. The grid cells for SI (30-m resolution) and LST (120-m resolution) that were contained completely within and intersected the corresponding buffer were included in the calculation. The zonal-stats operation was used to generate the average LST and SI for each of the buffers. Spearman rank correlation coefficients were calculated between the mean LSTs and SIs and the temperatures from the outdoor monitoring network averaged over 5 time periods: 12:05 pm [to correspond to the time of the satellite image, (average of 12:00 and 12:10 pm)];

average temperature from 9:20 am to 12:10 pm (3-hr average); average temperature from 4:00 to 5:00 am on 8/19/09 (nighttime temperature); average temperature from 12:10 pm on 8/18/09 to 12:10 pm 8/19/09 (daily); and, August average monthly temperature (monthly). The maximum and minimum temperatures and standard deviation for each group of measurements were calculated. These different time periods were chosen to see whether LST and/or SI taken at one point of time would give a better picture of instantaneous vs. longer-term spatial variation in temperatures in the study area.

Related to this point, we explored how representative the LST captured by the one usable 2009 LST image was of LST over a longer time frame, especially in this region where population growth and economic development have been static or declining in recent years. To better understand if the 2009 scene showed a similar spatial variation of temperatures within the region as other images from different time points and different years, multiple LST images from a 10-year time span were processed and evaluated in the same manner as the 2009 image. From the years 1999 to 2009, we found only 4 'high quality' images for the years 2002, 2003, 2004 and 2008, during our study months of June-August 31st. Correlation coefficients were calculated comparing a composite image (i.e. all 5 usable LST scenes overlaid in GIS) versus each single year scene. Additionally, the entire LST scenes (i.e. all 245,188 pixels, 120 m resolution) were used for this analysis, not just the temperatures extracted at the various buffers around the HOBO monitors.

SAS v 9.2 (SAS Institute, Cary, NC) was used for all statistical analysis and ArcGIS 9 was used for all spatial analysis.

RESULTS

Temperature data from 19 out of 24 ground-based monitors positioned throughout the county were used in the analysis. Five of the temperature monitors were excluded due to siting conditions that could have jeopardized the readings, such as being too close to a building. A search in the Landsat 4 and 5 TM archive datasets for the Detroit, Michigan area (latitude 42.331427, longitude -83.0457538), yielded a total of 21 satellite images. Out of these 21 images, 17 had a cloud cover percentage greater than 14%, and 16 did not cover the study area geographically. Consequently, 1 image, taken by the satellite on August 19, 2009, met our criteria (i.e., covered the geographic area of interest; had cloud cover of less than 14%, captured during the time period of the study (June 13 – September 30, 2009). This image was acquired during the daytime at 16:05 GMT (12:05 PM EDT). The quality of band 6 was scored as a 9, the highest score for images. This value reflects the quality and level of errors detected in the image. (Explanation can be found at <http://earthexplorer.usgs.gov/>). Figure 2 shows the final processed band 6 image of the study area.

The highest levels of mean SI were seen in the 500-m buffer zones across all of the locations (Table 1). Overall, the New Center location had the highest SIs (min-max range: 42 to 87.7%), and the New Boston location had the lowest overall SIs (min-max range: 9.0 to 18.5%). The New Center area location had the highest LSTs compared to other locations, from 24.4 to 25.6 °C, while the New Boston area had the lowest overall LSTs, from 18.2 to 18.4 °C. In terms of the ground based temperature readings, the instantaneous 12:05 pm time point at each location showed a higher max temperature than the other recorded time points.

At least two statistically significant correlations, for each radius distance, were seen between LST and the ground-based temperatures for the daily and monthly temperature for all buffers except 100 m, as shown in Table 2. At least three statistically significant correlations were also seen for each radius distance between SI and ground-based air temperature measurements for the time periods for nighttime temperature, daily temperature and monthly temperature at all buffers except the 0-m point. For the relationship between SI and LST, statistically significant correlations were found with Spearman correlation coefficients ranging from 0.49 to 0.91, as shown in Table 3.

In the analysis comparing spatial variation in LST using 5 summertime satellite images from the years 2002, 2003, 2004, 2008, and 2009, LST temperature ranges and the areas with the highest temperatures were consistent over the years. The 2009 LST scene was highly correlated with the 5-year composite LST scene ($R^2=0.96$). We also found a high correlation between the SI scenes from 2 different years, 2001 and 2006 ($R^2=0.98$).

DISCUSSION

The purpose of this study was to assess the relationship between LST and SI measurements and ground-based air temperature measurements in the Detroit Metropolitan Region. Our results showed a statistically significant relationship between LSTs and SI at all buffers, as well as LSTs and SIs and the ground-based air temperatures at certain buffers. These correlations between LST and SI are consistent with findings from other published studies (Cheung 2002; Imhoff et al. 2010; Zhou and Shepherd 2009; Uejio et al. 2011; Yuan and Bauer 2007). This suggests that SI data, which requires much less processing compared to the LST data, could be used as a proxy for LST. Consequently, public health researchers and practitioners may still be able to use a

fairly straightforward method to determine city hot-spots using high SI as an indicator of potential increased temperature exposure.

Our study used standard methods which facilitate comparisons with other work, and is the first analysis of this kind during the summer time in an large, urban Midwest city. Detroit has unique features, including a higher proportion of vacant lots than other metropolitan areas. Additionally, our study simultaneously explored the relationship between SI, LST calculated from thermal imagery, and ground-based temperature measures, adding the ‘ground-truthing’ element that has been called for to independently validate the satellite imagery as a proxy for human scale exposures (Voogt and Oke 2003).

The consistency of our findings with other studies suggest that these unique features do not impair the overall utility of satellite imagery for public health applications. In Detroit, the 2009 satellite-derived LST image—corrected for atmospheric effects and spatial variations in emissivity—as well as the SI image from the 2006 NLCD might be suitable to represent air temperature variability between sites for heat exposure studies in the region or for targeting heat-health interventions. Because our land-cover data does not distinguish among different types of impervious surface, we were unable to represent possible differences in emissivities among them and this is a type of variability that contributes to possible uncertainties in our analysis. The analysis we did comparing the 2009 scene with LST calculated from 4 previous years' summertime scenes showed that the LST estimated from the satellite images was relatively consistent over time, suggesting that changes in land use were not substantial in the Detroit Metropolitan Region. Further, for application in heat-health studies, LST is better suited for representing physical properties that are stable over time and can affect human temperature exposure rather than as a proxy for actual ambient air temperature at a particular point in time.

Our results complement those of two sister studies of the Detroit Metropolitan Area examining spatial variation of temperature during the entire summer of 2008. The first study used the same observational network of air temperature monitors used in the present study in conjunction with airport temperature monitors and monitors operated by the state of Michigan Department of Environmental Quality (Oswald et al. 2012). This study found the correlation between summer mean daily low temperature anomalies (the daily residuals at each location minus measurement uncertainty) in 2009 and SI in 2001 ($r = 0.68$ at the 200-m buffer, $p < 0.001$) to be higher than between daily temperature anomalies and other geographic characteristics. This suggests that in relatively sprawling cities, the urban heat island most closely follows SI and would have a unique structure in each city based on the SI structure (Oswald et al. 2012). A second study used geo-spatial approaches to create a continuous, spatial layer of estimated air temperature and found high correlations between SI measured in 2006 and observed air temperatures in 2008 (Zhang et al. 2011). Neither of those two studies examined LST, but the fact that they observed correlations between SI and air temperatures using different methodologies supports our finding that SI and, by extension, LST are moderately correlated with air temperature.

Previous studies have ground-truthed L5-TM data using airborne thermal scanner flights (Voogt and Oke 1998), or using satellite data in conjunction with ground-based air temperature measurements with other remote sensing predictors to create a model for air temperature (Cristobal et al. 2008). Other researchers have also created a spatio-temporal general linear model to estimate surface temperature using several predictors with 15 LANDSAT multispectral images taken between 1987-2002 for the Quebec Province, Canada, spanning the months of June to the end of August (Kestens et al. 2011). Using ambient temperatures recorded from multiple meteorological stations, they found that the 3-day average air temperature was a strong predictor

of LST, as well as the normalized difference vegetative index (NDVI) and land cover categories. Their results suggest that increasing the number of meteorological and geographical predictors could provide more precise estimates of heat exposure in urban areas.

An added benefit of using SI as a proxy for temperature exposure is that increasing vegetative cover and other changes can reduce the heat-trapping potential of the urban landscape, so results of studies using SI could be of direct relevance for policy changes. This finding might be helpful in the urban planning sector.

Correlations between LST and ground-based temperature measurements (Table 2), were stronger at the largest radii (e.g. 500 m and 800m), and stronger using the average temperature from day 1 to day 2 and the monthly temperature. Several possible reasons for this come to mind. Urban areas are heterogeneous in topography, physical structures, land use, etc. so ‘averaging’ of the LST temperature over a larger buffer zone may ‘drown’ out the physical noise that can influence the air temperature at a specific point.

The stronger correlations when temperatures are averaged over longer time spans suggest that instantaneous temperatures are less indicative of the overall spatial pattern of the temperature tendencies. Morning temperatures are likely less correlated due to lack of turbulent transport (the main mechanism relating source area to sensor) and influence of cold air drainage (i.e. topography). However, in terms of estimating personal exposure, lower correlation between these satellite data sources and the actual ground-based air temperature readings at 12:05 pm and the 3-hour average underscores the importance of identifying other tools that can better gauge actual short-term temperature exposure near the ground surface, especially when health outcomes that can result from acute exposures are of interest. Previous epidemiologic studies of

heat and daily mortality that have included Detroit have found that heat exposure on days 0-1 have been most relevant (e.g., Anderson and Bell 2009), though heat wave durations of at least 4 days may have an additional effect (e.g., Gasparinni and Armstrong 2010). The day is the common time unit of analysis for administrative databases of health outcomes (hospitalization, deaths, births), but other clinical outcomes that could be affected by heat (e.g., blood pressure, pulse rate) may be available at a finer time scale, such that hour-specific temperature data would be relevant. Longer duration of warm temperatures could also be relevant to both the exposure and the health resilience of residents, relating to air conditioning use and overall energy demand in homes.

Using the LST and SI data in conjunction with health outcome data could provide a more general understanding of spatial heat vulnerability. For example, an epidemiological investigation of a 1993 extreme heat event in Philadelphia used satellite imagery and geostatistical methods to determine if vulnerability to heat-related mortality was higher in areas with higher urban heat intensity (Johnson and Wilson 2009). They found that the heat load of the environment detected by the Landsat satellite data was potentially a contributing factor to heat-related deaths during the summer of 1993, and that the thermal data used in this study could be used to develop models of place-based vulnerability..

More frequent daily observations are made by MODIS. However, this sensor records thermal emission at a spatial resolution (1-km) too coarse for micro-urban heat island investigations. Future studies should investigate the public-health implications of this trade-off between temporal frequency and spatial resolution. Additionally, researchers have created new methods to better utilize satellite imagery to assess land surface temperature. In particular, physical and statistical methods for downscaling MODIS scenes (Liu and Pu 2008), and enhanced physical

methods that will reduce downscaling uncertainty, reduce the smooth effects and block effects due to isothermal assumption (Liu and Zhu 2012) could be incorporated into health studies.

Our ground-based temperature monitors were mounted 1.5 m above the ground, and the non-statistically significant relationships that we found between LST and the ground-based temperature monitoring network—for all buffers for the instantaneous and 3-hour average temperatures as well as the 0-700- m buffers for average daily temperature—might be a result of mixing, advection, and convection processes within the boundary layer that influence the air temperatures recorded by the outdoor temperature monitor. Since we are comparing two different types of measurements—surface temperature and air temperature—the correlations between these measurements might not be as strong, due to logistical (e.g. timing and resolution), as well as physical (e.g. advection, wind) considerations that could impact the derived surface temperatures.

Limitations

The availability of satellite products is a key limitation. Out of 21 LST scenes examined, only one scene was usable in that it lacked significant cloud cover and covered the study area geographically. The 16-day cycle on which Landsat images are acquired for a specific area does not afford researchers the opportunity to compare multiple images within a useful timeframe. Additionally, L5-TM data has a large spatial resolution (120 m), which might not capture the full heterogeneity of an urban environment (Johnson 2009).

Further, although we were able to match the time of acquisition of the ground data to the same time as the satellite data, the 12:05 pm passing time of the Landsat satellite is not optimal for temperature-health studies. First, this time generally corresponds to a time of the day when

ground temperatures transition from being cooler than air temperature to being warmer than air temperature. This means that, within the diurnal cycle, surface temperatures are not as significant drivers of air temperatures as they are later in the day. Second, exposure studies have tended to focus on maximum and minimum temperatures and this time corresponds with neither of these (Basu 2009). While shorter term ground based temperature timeframes did not yield strong correlations with SI or LST, composites of older satellite images could be one input into a more comprehensive planning tool or index to help describe vulnerability.

CONCLUSIONS

Our results support the need for an increased effort, nationally, by public and private entities, to create useful remotely-sensed data sources that can be applied to public health practice. A workshop report from the National Academy of Sciences (NAS 2007) discussed the challenges and potential applications of using remotely sensed data for public health. The report indicated that one of the major challenges to applying this remotely sensed data in the health arena is the limited in situ ground-truthing data accompanying remote sensing technology to verify analysis, and the high learning curve to using the tools required to analyze remotely sensed data. Our study gathered “ground-truthing” data needed to validate satellite derived LST as well as SI. However, our results highlight that issues of spatial resolution, image availability over certain time periods and the complex urban landscape remain challenges in the effort to integrate remotely sensed data with public health research and practice.

From a public health perspective, it is important to target resources and health interventions for the most vulnerable populations. The availability and usefulness of remote sensing data, integrated with social and economic demographic data, can provide a powerful tool

for assessing vulnerability. A quality of life study conducted by Athens-Clarke County used one cloud-free image, aerial photographs and U.S. Census data to overlay biophysical (land surface temperature, NDVI, land use and land cover) and socioeconomic layers (population density, per capita income, median home value, education) to create a quality of life indicator (Lo and Faber 1997). The research found a strong relationship between biophysical and socioeconomic variables, which could be useful to assess vulnerability in the public health arena. In the field of heat epidemiology, being able to utilize a user-friendly data source, like SI as a proxy for surface temperature exposure, can further our understanding of spatial vulnerability to heat. Another study has already shown that areas of the Detroit Metropolitan Region with high SI had statistically significant correlations with several socio-demographic variables: being age 65 years and older living alone, being able to leave the home, education level, living below the poverty line and being non-White (White-Newsome et al. 2009).

There are several ways that remote sensing data could be better integrated into public health practice: 1) increasing the capture frequency of remotely sensed images available for research and planning purposes; 2) providing more highly processed data accessible to the public, at a finer resolution (10-15 m) and if possible at a higher temporal frequency that could be more useful for city and county level authorities; 3) Commissioning more research to ground-truth satellite-derived land surface temperatures for different sized urban areas, and establishing a set of fairly simple, standard best practices that can be used to estimate the influences of atmospheric and other factors on deriving a precise LST value from remote sensed imagery could be useful for planning for extreme heat events. Landsat data are the most consistent and widely available source of relatively high-resolution thermal information from satellites, but can be limited due to the number of clear images available at certain days and times. A gap in

availability of these data exists, but continued acquisition of these data or data of comparable resolution has the potential to provide important spatial information about differential heat exposures.

One contribution of this particular study is important is to underscore the importance of the limitations of data, especially and to offer the perspective that it is critical to have data that is accessible, useful and timely for those working in the field of public health. One of the main objectives of this study was to see if a “non remote-sensing professional” could create a tool – using available data - that can be used to estimate heat exposure. Reporting on the challenges we faced in doing this is one way to bring the issue to the attention of the remote sensing community. The more practitioners demand the availability and need for this data, we hope that our research and other research that attempts to use the ‘simplest methods’ can provide the impetus to fill this well-known gaps in data needs overcome these limitations.

REFERENCES

- Anderson, G. B. and M. L. Bell. 2009. Weather-related mortality: A study of how heat, cold, and heat waves affect mortality in the United States. *Epidemiology* 20(2):205-213.
- Aniello C, Morgan K, Busbey A, Newland L. 1995. Mapping micro-urban heat islands using Landsat TM and GIS. *Comput Geo Sci* 21(8):335-344.
- Atmospheric correction parameter calculator. Barsi, J.A., J.L. Barker, J.R. Schott. An Atmospheric Correction Parameter Calculator for a Single Thermal Band Earth-Sensing Instrument. IGARSS03, 21-25 July 2003, Centre de Congres Pierre Baudis, Toulouse, France. Available: <http://atmcorr.gsfc.nasa.gov/> [accessed 27 May 2013].
- Basu R. 2009. High ambient temperature and mortality: a review of epidemiologic studies from 2001 to 2008. *Environ Health* 8:40 doi:10.1186/1476-069X-8-40.
- Chander G, Markham BL, Helder DL. 2009. Summary of current radiometric calibration coefficients for Landsat MSS, TM, ETM+, and EO-1 ALI sensors. *Remote Sens Environ* 113(5): 1-24.
- Cristóbal J, Ninyerola M, Pons X. 2008. Modeling air temperature through a combination of remote sensing and GIS data. *J Geophys Res* 113:13.
- National Academy of Sciences. 2007. Contributions of land remote sensing for decisions about food security and human health: workshop report. Available at: <http://www.nap.edu/catalog/11759.html>.
- Fung WY, Lam KS, Nichol J, Wong MS. 2009. Derivation of nighttime urban air temperatures using a satellite thermal image. *American Meteorological Society* 48:863-872.
- Gasparrini A, Armstrong B. 2010. The impact of heat waves on mortality. *Epidemiology* 22(1):68-73.
- Harlan SL, Deplet-Barreto JH, Stefanov WL, Petitti DB. (2013). Neighborhood effects on heat deaths: social and environmental predictors of vulnerability in Maricopa County, Arizona. *Environ Health Perspect* 121(2):197–204. doi: 10.1289/ehp.1104625
- Imhoff ML, Zhang P, Wolfe RE, Bounoua L. 2010. Remote sensing of the urban heat island effect across biomes in the continental USA. *Remote Sensing of Environment* 114(3): 504–513.

- Johnson DP, Wilson JS. 2009. The socio-spatial dynamics of extreme urban heat events: The case of heat-related deaths in Philadelphia. *Appl Geogr* 29(3):419-434.
- Johnson DP. 2009. Geospatial technologies for surveillance of heat related health disasters. In: *Planning and Socioeconomic Applications, Vol 1: Netherlands, Springer*, 139-154.
- Kalkstein LS, Greene JS. 1997. An evaluation of climate/mortality relationships in large U.S. cities and the possible impacts of a climate change. *Environmental Health Perspectives* 105: 84-93.
- Kestens Y, Brand A, Fournier M, Goudreau S, Kosatsky T, Maloley M, et al. 2011. Modeling the variation of land surface temperature as determinant of risk of heat-related health events. *Int J Health Geogr* 10(7):1-9.
- Lillesand TM, Kiefer RW, Chipman JW. 2004. *Remote sensing and image interpretation*. New York: John Wiley & Sons, Inc.
- Liu D, Pu R. 2008. Downscaling thermal infrared radiance for subpixel land surface temperature retrieval. *Sensors* 8:2695-2706.
- Liu D, Zhu X. 2012. An enhanced physical method for downscaling thermal infrared radiance. *IEEE Geoscience and Remote Sensing Letters*:9:690-694.
- Lo CP, Quattrochi DA. 2003. Land-use and land-cover change, urban heat island phenomenon, and health implications: A remote sensing approach. *Photogrammetric Engineering and Remote Sensing* 69:1053-1063.
- Lo CP, Faber BJ. 1997. Integration of landsat thematic mapper and census data for quality of life assessment. *Remote Sens Environ* 62(2):143-157.
- MRLC (Multi-Resolution Land Characteristics Consortium). 2013. National Land Cover Database 2006. Available: <http://www.mrlc.gov/nlcd2006.php> [accessed 27 May 2013].
- NASA (National Aeronautics and Space Administration). 2011. MODIS. Available: <http://modis.gsfc.nasa.gov/about/> [accessed 27 May 2013].
- NASA Jet Propulsion Laboratory California Institute of Technology. 2012. ASTER. Available: <http://asterweb.jpl.nasa.gov/> [accessed 27 May 2013].
- O'Neill MS, Zanobetti A, Schwartz J 2003. Modifiers of the temperature and mortality association in seven US cities. *American Journal of Epidemiology* 167:1074-1082
- O'Neill MS, Zanobetti A, Scwartz, J. 2005. Disparities by race in heat-related mortality in four US cities: The role of air conditioning prevalence. *Journal of Urban Health* 82:191-197.

ONSET HOBO Data Loggers. 2013. Available:

http://www.onsetcomp.com/files/manual_pdfs/10694-K-MAN-U23.pdf [accessed 27 May 2013].

Oswald E, Rood RB, Zhang K, Gronlund C, O'Neill MS, White-Newsome JL, et al. 2012. An investigation into the spatial variability of near-surface air temperatures in the Detroit, MI metropolitan region. *J Appl Meteor Climatol* 51:1290-1304.

Rigo G, Parlow E, Oesch D. 2006. Validation of satellite observed thermal emission with in-situ measurements over an urban surface. *Remote Sens Environ* 104:201-210.

Roy SS, Yuan F. 2009. Trends in extreme temperatures in relation to urbanization in the twin cities metropolitan area, Minnesota. *American Meteorological Society* 48:669-679.

Schwartz J, Samet JM, Patz JA. 2004. Hospital admissions and heart disease: the effects of temperature and humidity. *Epidemiology* 6:755-761.

Sheridan S, Kalkstein A. 2010. Seasonal variability in heat related mortality across the United States. *Natural Hazards* 55:291-305.

Uejio C K, Wilhelmi OV, Golden JS, Mills DM, Gulino SP, Samenow, JP. 2011. Intra-urban societal vulnerability to extreme heat: The role of heat exposure and the built environment, socioeconomics, and neighborhood stability. *Health Place* 17(2):498-507.

USGS (U.S. Geological Survey). 2013. Earthexplorer. Available: <http://earthexplorer.usgs.gov/>. [Accessed 27 May 2013].

Voogt JA, Oke TR. 1998. Effects of urban surface geometry on remotely-sensed surface temperature. *Int J Remote Sensing* 19(5):895-920.

Weng Q. 2009. Thermal infrared remote sensing for urban climate and environmental studies: methods, applications, and trends. *ISPRS Journal of Photogrammetry and Remote Sensing* 64 (4):335-344.

White-Newsome JL, O'Neill MS, Gronlund C, Sunbury T, Parker EA, Brown DG, et al. 2009. Climate change, heat waves and environmental justice: advancing knowledge and action. *Environmental Justice* 2(4):197-205.

WMO (World Meteorological Organization). 2008. Guide to Meteorological Instruments and Methods of Observation, Chapter 2: Measurement of Temperature. Available at: http://www.wmo.int/pages/prog/gcos/documents/gruanmanuals/CIMO/CIMO_Guide-7th_Edition-2008.pdf. [accessed 27 May 2013].

- Yuan F, Bauer ME. 2007. Comparison of impervious surface area and normalized difference vegetation index as indicators of surface urban heat island effects in Landsat imagery. *Remote Sens Environ* 106:375-386.
- Zhang K, Oswald EM, Brown DG, Brines SJ, Gronlund CJ, White-Newsome JL, et al. 2011. Geostatistical exploration of spatial variation of summertime temperatures in the Detroit metropolitan region. *Environ Res* 111(8):1046-1053.
- ZhouY, Shepherd JM .2009. Atlanta's urban heat island under extreme heat conditions and potential mitigation strategies. *Natural Hazards* 52(3):639–668.

Table 1. Summary of satellite-derived average land surface temperature (LST) measurements and ground-based temperature monitoring network temperatures.

Location Name	Percent surface imperviousness at different radii (in meters) around the outdoor monitoring point						Landsat derived surface temperatures (°C) at different radii (in meters) around the outdoor monitoring point						Ground based temperature network readings (°C)				
	0	100	300	400	500	800	0	100	300	400	500	800	Sat ^a	3-hr avg ^b	Night ^c	Daily avg ^d	Monthly avg ^e
Allen Park	13.0	29.3	51.5	50.9	47.9	44.8	21.6	21.3	22.2	22.3	22.3	21.8	26.5	25.3	19.6	24.0	21.7
Canton	59.0	33.8	36.3	36.2	37.1	35.5	21.1	21.4	21.8	22.0	21.9	21.7	25.6	24.4	17.1	22.2	20.7
Conner	69.0	64.1	75.1	74.3	74.8	73.4	23.4	23.1	22.7	23.0	23.1	23.7	26.3	25.2	18.8	24.4	22.0
Corktown	35.0	48.9	48.8	53.0	59.7	65.8	21.1	21.6	22.1	22.4	22.9	23.4	27.6	25.6	19.0	23.7	21.7
East Detroit	61.0	71.0	50.4	52.2	53.4	54.5	22.1	21.8	21.2	21.3	21.3	21.4	26.2	24.9	20.4	24.4	22.0
East Jefferson	32.0	37.0	41.1	44.5	45.1	49.1	19.2	19.2	19.7	20.0	20.1	20.4	23.5	23.4	19.3	23.2	20.9
Garden City	47.0	50.5	50.8	51.1	51.9	52.7	22.0	22.0	21.8	22.0	22.2	22.3	26.7	23.9	18.8	23.4	21.3
Indian Village	58.0	42.2	41.2	43.5	47.0	51.2	20.4	20.3	20.1	20.4	20.7	21.2	26.7	23.3	19.8	23.8	21.7
Joy Rd	35.0	19.6	15.1	13.3	12.2	13.7	20.8	21.0	19.6	19.1	18.9	19.0	26.7	25.3	18.2	23.3	21.1
New Boston	9.0	9.0	18.5	18.3	16.8	13.9	18.6	18.4	18.4	18.4	18.4	18.4	27.3	25.5	18.3	22.6	20.9
New Center	42.0	79.2	86.1	87.4	87.7	83.1	24.9	25.6	25.5	25.2	24.9	24.4	26.7	25.1	21.0	24.8	22.3
Redford2	44.0	49.7	55.7	55.6	56.5	57.0	22.6	22.9	22.8	22.7	22.6	22.4	24.8	24.7	19.3	23.8	21.5
UM Dearborn	14.0	39.1	35.3	37.1	37.5	33.9	21.3	21.2	21.5	21.1	21.1	20.5	26.1	24.8	18.2	23.0	21.1
West Detroit 1	25.0	45.0	43.7	43.3	45.8	51.0	20.8	20.9	21.1	21.2	21.4	21.8	25.1	23.7	19.7	23.6	21.5
West Detroit 3	57.0	66.4	69.6	65.6	62.5	57.3	23.5	23.6	23.3	22.9	22.5	22.2	28.0	24.0	19.7	24.0	21.5
West Detroit 5	55.0	54.4	50.0	53.3	55.8	62.3	21.2	21.1	21.5	21.7	22.0	22.5	27.7	26.4	18.9	23.5	21.6
West Village	30.0	45.0	51.8	50.5	48.1	50.7	20.5	20.5	20.7	20.9	20.9	21.3	26.7	25.3	19.9	24.1	21.7
Westland	84.0	47.4	45.2	47.5	45.3	38.5	24.7	23.9	22.3	22.1	21.7	21.0	26.5	23.2	18.4	23.1	21.2
Wayne State University	32.0	76.1	81.5	75.0	70.9	71.5	23.1	23.7	24.1	23.9	23.6	23.5	26.7	25.3	20.1	24.2	22.0
Min	9.0	9.0	15.1	13.3	12.2	13.7	18.6	18.4	18.4	18.4	18.4	18.4	23.5	23.2	17.1	22.2	20.7
Max	84.0	79.2	86.1	87.4	87.7	83.1	24.9	25.6	25.5	25.2	24.9	24.4	28.0	26.4	21.0	24.8	22.3
Standard Deviation	20.1	18.4	18.5	17.9	17.9	18.1	1.7	1.7	1.7	1.6	1.5	1.5	1.1	0.9	0.9	0.6	0.4

^aSat: instantaneous satellite temperature taken at 12:05 ^b3-hr Avg: average temperature from 9:20 am to 12:10 pm PM. ^cNight: average nighttime temperature from 4:00 to 5:00 am on 8/19/2009 ^dDaily Avg: average temperature from 12:10 pm on 8/18/09 to 12:10 pm 8/19/2009 ^eMonthly Avg: August average monthly temperature

Table 2. Spearman rank correlation coefficients and p-values between satellite-derived land surface temperature (LST) and surface imperviousness measurements (SI), with ground-based temperature measurements.

Measurement	Concentric radii distances around monitoring point used to calculate an average	Ground-based Temperature Measurements				
		Instantaneous 12:05 PM Temperature on 8/19/2009	Average temperature from 9:20 am - 12:10 pm	Average Temperature from 4:00 to 5:00 am on 8/19/2009	Average Temperature from 12:05 pm to 12:10 pm 8/19/2009	August Average Monthly Temperature
LST	At Point (0 m)	0.0018 (0.99)	-0.11 (0.66)	0.22 (0.36)	0.47 (0.043)	0.47 (0.041)
	100 meters	0.026 (0.91)	-0.10 (0.68)	0.21 (0.38)	0.44 (0.060)	0.44 (0.053)
	300 meters	0.0070 (0.98)	-0.0070 (0.98)	0.28 (0.24)	0.48 (0.038)	0.51 (0.027)
	400 meters	0.030 (0.90)	0.084(0.73)	0.33 (0.17)	0.55 (0.015)	0.59 (0.0084)
	500 meters	0.068 (0.78)	0.18 (0.45)	0.32 (0.18)	0.55 (0.014)	0.61 (0.0057)
	800 m	0.13 (0.60)	0.25 (0.30)	0.41 (0.085)	0.62 (0.0048)	0.68 (0.0014)
SI	At Point (0 m)	0.058 (0.81)	-0.39 (0.098)	-0.0097 (0.97)	0.17 (0.47)	0.71 (0.48)
	100 meters	0.16 (0.50)	0.019 (0.94)	0.59 (0.0075)	0.72 (0.0005)	0.69 (0.001)
	300 meters	0.081 (0.74)	0.15 (0.54)	0.66 (0.002)	0.83 (<0.0001)	0.81 (<0.0001)
	400 meters	0.17 (0.48)	0.20 (0.40)	0.59 (0.0077)	0.76 (0.0001)	0.77 (0.0001)
	500 meters	0.22 (0.36)	0.22 (0.36)	0.62 (0.0043)	0.81 (<0.0001)	0.82 (<0.0001)
	800 meters	0.22 (0.37)	0.17 (0.48)	0.60 (0.0062)	0.75 (0.0002)	0.77 (0.0001)

Spearman correlation statistical test was used to calculate a correlation coefficient. P values < 0.05 denote significance. -

Table 3. Spearman rank correlation coefficients (r) between satellite-derived land surface temperature (LST) and percent surface imperviousness (SI).

LST vs. SI calculated at the following concentric radii (meters)	r (p-value)
0 (at the point)	0.49(0.032)
100	0.74(0.003)
200	0.74(<0.0003)
300	0.79(<0.0001)
400	0.84(<0.0001)
500	0.86(<0.0001)
800	0.91(<0.0001)

Figure Legends

Figure 1. Flowchart that describes the processing method for converting raw satellite images to land surface temperature. Parallelograms denote data inputs, squares denote calculations and the shaded oval denotes the final value (temperature leaving the earth's surface).

Figure 2. Final processed Landsat-5 TM image of the Detroit Metropolitan Region study area and the locations of the ground-based temperature monitors (HOBOS).

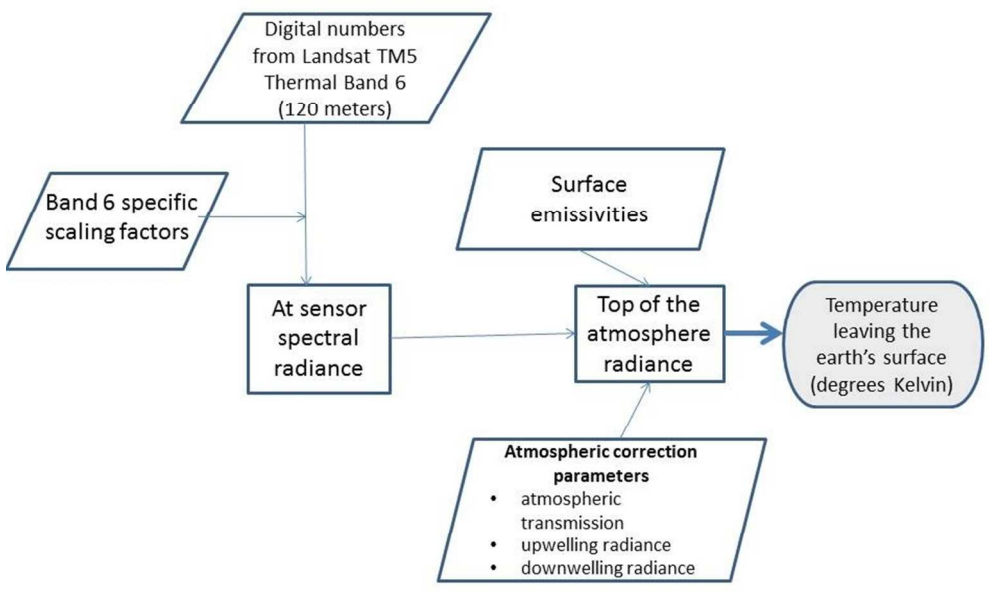


Figure 1
254x190mm (96 x 96 DPI)

